

Passive and semi-active control of an offshore floating wind turbine using a tuned liquid column damper

Christophe Coudurier* Olivier Lepreux* Nicolas Petit**

* *IFP Energies nouvelles, Rond-point de l'échangeur de Solaize, BP 3, 69360 Solaize, France, e-mails: christophe.coudurier@ifpen.fr, olivier.lepreux@ifpen.fr*

** *MINES ParisTech, Centre Automatique et Systèmes, Unité Mathématiques et Systèmes, 60 Bd St-Michel, 75272 Paris, Cedex 06, France, e-mail: nicolas.petit@mines-paristech.fr*

Abstract: Offshore floating wind turbines seem a promising technology to harvest wind energy in deep waters. In order to be economically viable it requires mitigating the mechanical loads induced by the waves. This paper shows that the tuned liquid column damper (TLCD) technology, currently employed in naval engineering can be of great relevance to address this issue, if combined with a control strategy. The control strategy consists in adapting the damping coefficient of the TLCD in real time. The performance obtained with the optimal constant damping coefficient serves as a reference to assess the possible improvements brought by active technologies. Simulation conducted in this article report a 39% reduction of the pitch oscillations on a typical 5000 tonnes barge excited by a JONSWAP irregular wave.

© 2015, IFAC (International Federation of Automatic Control) Hosting by Elsevier Ltd. All rights reserved.

1. INTRODUCTION

Wind power is the second fastest growing renewable source of electricity (National Renewable Energy Laboratory, 2012) in terms of installed power. All over the world, constructions of offshore wind farms are booming. According to the 2012 GWEC annual report (Fried et al., 2012), production facilities summing up to a total of 80 GW are expected to be installed by 2020 worldwide. Root causes for this recent trend are the strength and regularity of wind far from the shore, which, in principle, grant easy production of electricity. To recover offshore wind energy, two main technologies are considered: fixed-bottom wind turbines (having foundations fixed into seabed) and floating wind turbines (FWT). Fixed bottom offshore wind turbines reveal too costly for waters deeper than 60 m (Musial et al., 2006), which discards them from most interesting fields. The FWT is a tempting alternative. On the up side, installation of FWT is little dependant on seabed conditions, and FWT can be moved to harbour for maintenance. On the down side, the main drawback of FWTs is their sensitivity to surrounding water waves causing the wind turbine to undergo heavy mechanical loads (Jonkman, 2007), which reduce their lifespan. This sensitivity can be attenuated by increasing the mass and stiffness of the structure. However, this apparently straightforward solution raises the cost per kWh in a prohibitive manner. In this article, we consider an alternative solution.

Previous works have proposed to compensate tower fore-aft oscillations using collective and individual blade pitch control to modify the wind thrust forces (Jonkman, 2007; Namik, 2012; Christiansen et al., 2013). It is explained that blade pitch control can not reduce platform movement and tower loads at the same time. Further, blade pitch control

already has to pursue other objectives such as generator torque and speed control. This is why this solution has very limited performance, and tower movements are still many times larger than what is observed on onshore wind turbines. Instead of using aerodynamic forces, it is tempting to consider using hydrodynamic ones. In naval engineering, this is an approach used to damp ship roll. However, most solutions use the speed of the ship relatively to the water to generate lift to control roll (Perez and Blanke, 2012) and, for this reason, are not easily transferable to our problem. To reduce pitch oscillations, we study an alternative way to act on the floater motion. This paper is focused on stabilizing FWT by means of an attached oscillating system.

The approach we advocate has its roots in earlier works. To improve the response of massive structures to external disturbances, attached moving masses such as Tuned Mass Dampers (TMD) have been employed. One of the most economical and efficient solution is the Tuned Liquid Column Damper (TLCD) also known as anti-rolling tank or U-tank. As originally proposed by Frahm (Frahm, 1911; Moaleji and Greig, 2007), it is a U-shaped tube, belonging to a plane orthogonal to the ship roll axis, generally filled with water. The liquid inside the TLCD creates a phase shift of the movement of the structure. The liquid energy is dissipated through a restriction located in the horizontal section. The TLCD is usually chosen to damp the natural frequency of the structure. Note that the TLCD can provide damping perpendicularly to the wind direction, unlike blade pitch control.

While modelling of TLCD system has been done in civil engineering in the past by e.g. (Chang and Hsu, 1998; Gao et al., 1997), it is still an active field of research (Di Matteo et al., 2014; Holden and Fossen, 2012). Most

efforts have been spent on determining optimal designs for passive TLCDs (Gao et al., 1997; Wu et al., 2009; Yalla and Kareem, 2000), and on developing active control strategies (Moaleji and Greig, 2006; Chen and Ko, 2003; Fu, 2011; Holden et al., 2009).

In our approach, we consider both the floater (which has no fixed point) and the TLCD, and study their mutual interactions. The first contribution of this article is a Lagrangian formulation of the free oscillations of the coupled system. The second novelty of our work is that we consider a semi-active TLCD, which restriction is variable. To use this degree of freedom, we develop a semi-active control strategy and evaluate its performance in a realistic set-up.

This paper is organized as follows. In Section 2, we present the governing equations. The system consisting in the floater, the wind turbine, and the TLCD has one input, the head loss resulting from the valve position, and is subject to an unmeasured disturbance, the wave force. A model is derived with 8 state variables. In Section 3, we study the open-loop response of the system to the wave force (the disturbance). We highlight the appearance of two resonant peaks. In addition, we show how the response is impacted by the (constant) value of the head loss coefficient. Employing a constant head-loss coefficient reveals a very limited solution as we highlight the existence of quasi-fixed points in the frequency response diagram. Then, in Section 4, we propose a *semi-active control* scheme. Using a state space representation and a classic LQR design, where the head-loss coefficient of the TLCD is controlled, we optimize the damping according to a feedback on the movement of the floater generated by the wave. The head-loss being limited in practice, a saturation of this input is taken into account. With this strategy, the magnitude of the oscillations is significantly reduced. The pitch oscillations of a 5000 tonnes floater subject to a JONSWAP irregular wave is reduced up to 37% with respect to the FWT without TLCD.

2. SYSTEM MODELLING

Without loss of generality, the floater under consideration in this study is the MIT/NREL Barge and the wind turbine is the NREL 5MW (Jonkman, 2007). The system is pictured in Fig.1. The wind turbine is considered as a rigid body, carried by the floater, which is modelled as a floating rigid body.

The system is studied in a vertical plane allowing only 3 DOFs: surge, heave, and pitch. Heave and pitch motions are coupled. The TLCD is modelled as a U-shaped pipe of cross-section equal to A_V in the vertical parts and A_H in the horizontal part. The variable restriction causing the damping (head loss) is located in the middle of the horizontal section. To avoid any bias in the study, we do not take the interaction between the rotor and the wind into account, (its impact could be negative or positive (Larsen and Hanson, 2007)).

Leaving out the water contained in the TLCD, the motion of the floater and the wind turbine can be modelled, with all its interactions with the water, with a high level

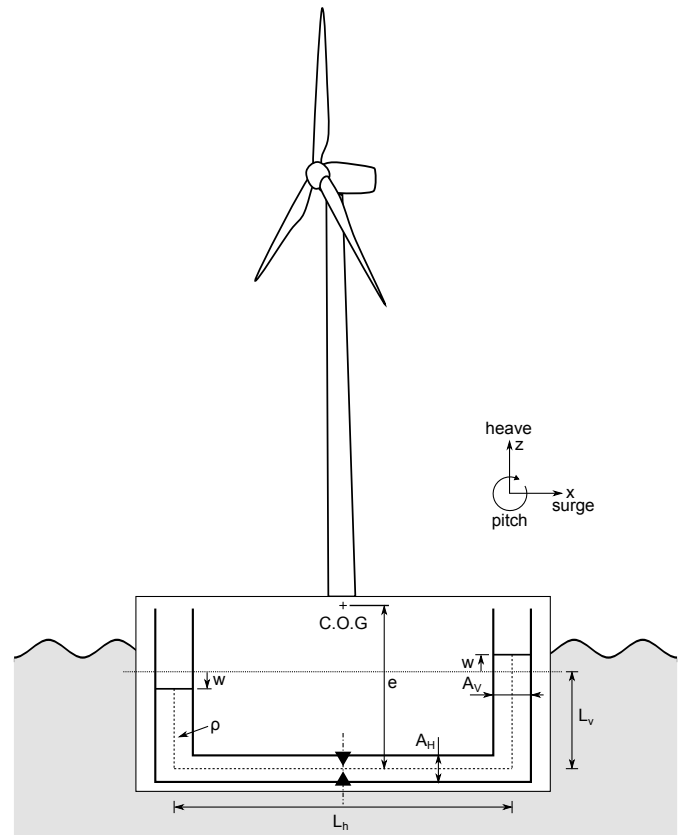


Fig. 1. Diagram of the floater with the wind turbine and the TLCD

of fidelity in a state-of-the-art hydrodynamics solver for floating systems, e.g. Diodore™.

2.1 Linear hydrodynamic model

For small incident waves, one can use the theory of linear hydrodynamics (Newman, 1977). In this theory, three independent phenomena occur simultaneously: (i) when the floater is slightly moved from its equilibrium position in a still sea, the water tries to restore the equilibrium, this phenomenon is known as *hydrostatics*; (ii) when the floating body is oscillating in calm waters, it creates a field of waves, this is known as the *radiation*; (iii) a steady floater is subjected to an incident wave field, which is modified by the presence of the floating body, it is called the *wave-excitation*. As a result, the equations of motion of the rigid part of the system are of the form

$$M_h \ddot{X}_h + K_h X_h = F(t) + F_{rad}(t, \dot{X}_h, \ddot{X}_h) \quad (1)$$

with

$$M_h = 10^6 \begin{bmatrix} 5.19 & 0 & 0 \\ 0 & 5.19 & 0 \\ 0 & 0 & 2750 \end{bmatrix} \quad K_h = 10^8 \begin{bmatrix} 0 & 0 & 0 \\ 0 & 1.01 & 0 \\ 0 & 0 & 39.1 \end{bmatrix}$$

M_h is the mass matrix in which the mass matrix of the floater M_B and the mass matrix of wind turbine M_{WT} (as given in (Jonkman, 2007)) appear, K_h is the matrix accounting for the hydrostatic stiffness. F is the wave-excitation force 3×1 vector (as described in (Newman, 1977)) and is time-varying, F_{rad} is the 3×1 damping force vector due to the radiation phenomenon. Finally $X_h = (x_G \ z_G \ \alpha)^T$ is a 3×1 vector describing the position of

the centre of gravity and the pitch angle α of the structure in the vertical plane under consideration. Usually the goal of the mooring system for a barge is just to prevent drifting (Butterfield et al., 2007). The mooring stiffness matrix is heavily dependent on the technology used, here we suppose that we use catenary mooring with parameters such that its effects on the dynamic behaviour of the barge are negligible.

Radiation forces In our approach, K_h , F and F_{rad} of (1) are determined using the hydrodynamics analysis software Diodore¹. Following (Newman, 1977), under steady conditions and in the case of a monochromatic wave, the radiation force can be simplified under the form

$$\tilde{F}_{rad} e^{i\omega t} = \tilde{X}_h e^{i\omega t} (\omega^2 A_h(\omega) - i\omega B_h(\omega)) \quad (2)$$

with $A_h(\omega)$ and $B_h(\omega)$ defined as the hydrodynamic added mass and the hydrodynamic damping, respectively. They are depending on ω the pulsation of the monochromatic wave. \tilde{X}_h and \tilde{F}_{rad} are complex magnitudes. These terms are calculated by Diodore, using a linear hydrodynamic model, for a vast collection (27) of different wave periods ranging from 3 to 120 s.

Noting $p = i\omega$, (2) rewrites in the Laplace domain

$$\tilde{F}_{rad} = -p\tilde{X}_h (pA_h(p) + B_h(p)) \triangleq -p\tilde{X}_h G(p) \quad (3)$$

In this equation $G(p)$ is approximated by a 3×3 matrix of biproper 5th order transfer functions to fit the data provided by Diodore in the frequency domain. From (1) and (3), an approximated model is built.

Morison's viscous drag As linear hydrodynamics equations lead to huge displacements at resonance, the assumption of linearity is not valid in this case. When oscillations of the floater become large, a phenomenon that we have neglected so far damps the floater much more than the radiation. This extra damping is due to viscous effects such as skin friction, vortices, etc. To account for this effect, we add the viscous-drag term from Morison's theory (Jonkman, 2007; Newman, 1977), this term quadratically depends on the speed. We update (1) as

$$M_h \ddot{X}_h + K_h X_h = F(t) + F_{rad}(t, \dot{X}_h) + F_{visc}(t, X_h, \dot{X}_h) \quad (4)$$

The relevance of the model has been assessed through a comparison against the full linear hydrodynamics simulation performed by the software Diodore. In these simulations, the platform is subjected to a polychromatic JONSWAP wave (Hasselmann et al., 1973).

2.2 Equations of motion

We now incorporate the water contained in the TLCD into the dynamics. The following assumptions are considered: (i) the in-plane width of the TLCD vertical column cross section is negligible compared to the horizontal length, and, similarly, the in-plane width of the TLCD horizontal column cross section is negligible compared to the vertical length, (ii) the fluid is incompressible, (iii) the liquid velocity is uniform in the horizontal and vertical columns.

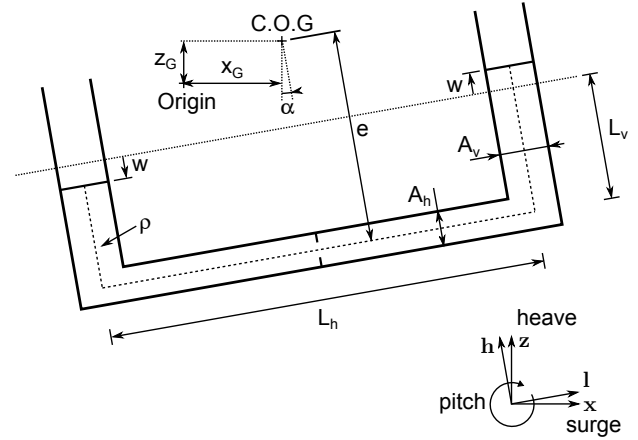


Fig. 2. Schematic diagram of the structure with the TLCD in motion.

We note $\mathcal{R} \triangleq (O, \mathbf{x}, \mathbf{y}, \mathbf{z})$ an inertial frame of reference and $\mathcal{R}_D \triangleq (G, \mathbf{h}, \mathbf{d}, \mathbf{l})$ a reference frame attached to the floater, centred on its centre of gravity. Classically, we note the kinetic energy T which is the sum of the kinetic energy of the structure noted T_S and the kinetic energy of the liquid contained in the TLCD noted T_D

$$T = T_S + T_D, \quad T_S = \frac{1}{2} \dot{X}_h^T M_h \dot{X}_h \quad (5)$$

The kinetic energy of the TLCD writes

$$T_D = \frac{1}{2} \mu_v \int_{-e}^{-e+L_v+w} \mathbf{v}_{RC}^2 dh + \frac{1}{2} \mu_v \int_{-e}^{-e+L_v-w} \mathbf{v}_{LC}^2 dh + \frac{1}{2} \mu_h \int_{-\frac{1}{2}L_h}^{\frac{1}{2}L_h} \mathbf{v}_{HC}^2 dl \quad (6)$$

with \mathbf{v}_{RC} , \mathbf{v}_{LC} , \mathbf{v}_{HC} being, respectively, the velocity of any fluid particle in the tube right, left, and horizontal column and expressed as

$$\mathbf{v}_{RC} = \dot{z}_G \mathbf{z} + \dot{x}_G \mathbf{x} + \dot{w} \mathbf{h} + \dot{\alpha} (h \mathbf{l} - \frac{L_h}{2} \mathbf{h}) \quad (7)$$

$$\mathbf{v}_{LC} = \dot{z}_G \mathbf{z} + \dot{x}_G \mathbf{x} - \dot{w} \mathbf{h} + \dot{\alpha} (h \mathbf{l} + \frac{L_h}{2} \mathbf{h}) \quad (8)$$

$$\mathbf{v}_{HC} = \dot{z}_G \mathbf{z} + \dot{x}_G \mathbf{x} + \nu \dot{w} \mathbf{l} - \dot{\alpha} (e \mathbf{l} + l \mathbf{h}) \quad (9)$$

and

$$\mu_v = A_V \rho \quad \mu_h = A_H \rho$$

The equations (5-9) are generalised expressions in the vertical plane of the calculus developed by (Wu et al., 2008) that considered only the pitching motion of a structure. As pictured in Fig.2, the variables z_G and x_G are the coordinates of the centre of gravity of the floater with respect to \mathcal{R} , α is the pitch angle of the floater, w is the liquid displacement, h and l are the coordinates of the fluid particle, respectively, along \mathbf{h} and \mathbf{l} axis. A_V (A_H) and L_v (L_h) are the cross-section area of the vertical (horizontal) part and the length of vertical (horizontal) column respectively, e is the distance between the centre of the horizontal part and the centre of gravity, ρ is the fluid density, and $\nu = A_V/A_H$ is the cross-section ratio.

Some lines of computation show that T_D can be rewritten as

¹ <http://www.principia.fr/expertise-fields-software-products-diodore-132.html>

$$\begin{aligned}
T_D = & \frac{1}{2}M_D(\dot{z}_G^2 + \dot{x}_G^2) + \frac{1}{2}J_D\dot{\alpha}^2 \\
& + \frac{1}{2}\mu_v L_e \dot{w}^2 - \mu_v (L_v + e) L_h \dot{w} \dot{\alpha} \\
& + (\dot{z}_G \cos \alpha + \dot{x}_G \sin \alpha) \mu_v w (2\dot{w} - L_h \dot{\alpha}) \\
& + (-\dot{z}_G \sin \alpha + \dot{x}_G \cos \alpha) \dot{\alpha} \\
& \quad (\mu_v (w^2 - L_v(2e - L_v)) - \mu_h L_h e) \\
& + \mu_v L_h \dot{w} (-\dot{z}_G \sin \alpha + \dot{x}_G \cos \alpha) \\
& + \mu_v ((L_v - e) w^2 \dot{\alpha}^2)
\end{aligned}$$

with the mass and the moment of inertia of the liquid being respectively

$$\begin{aligned}
M_D & \triangleq 2\mu_v L_v + \mu_h L_h \\
J_D & \triangleq \mu_h L_h \left(e^2 + \frac{1}{12} L_h^2 \right) \\
& \quad + 2\mu_v L_v \left(\frac{L_h^2}{4} + \frac{L_v^2}{3} - e L_v + e^2 \right)
\end{aligned}$$

and the equivalent length

$$L_e \triangleq 2L_v + \nu L_h$$

The potential energy of the system V can be written as the sum of the potential energies of the structure (due to the hydrostatic stiffness) and of the TLCD

$$V = V_S + V_D, \quad V_S = \frac{1}{2} X_h^T K_h X_h$$

where

$$\begin{aligned}
V_D = & M_D g z_G + \mu_h L_h g e \cos \alpha \\
& + \mu_v (L_v + w) g \left((L_v + w - e) \mathbf{h} + \frac{L_h}{2} \mathbf{1} \right) \cdot \mathbf{z} \\
& + \mu_v (L_v - w) g \left((L_v - w - e) \mathbf{h} - \frac{L_h}{2} \mathbf{1} \right) \cdot \mathbf{z}
\end{aligned}$$

which is directly rewritten as

$$\begin{aligned}
V_D = & \mu_v g \cos \alpha (w^2 - L_v(2e - L_v)) + M_D g z_G \\
& - \mu_v g L_h \sin \alpha w - \mu_h g \cos \alpha L_h e
\end{aligned}$$

where g is the acceleration of gravity. Without loss of generality, the point of zero potential energy has been chosen to be the centre of gravity of the structure.

The equations of motion of the system are obtained via a Lagrangian approach,

$$\frac{d}{dt} \left(\frac{\partial \mathcal{L}}{\partial \dot{q}_i} \right) = \frac{\partial \mathcal{L}}{\partial q_i} + f_i, \quad \mathcal{L} = T - V$$

where the non-conservative forces f_i applied to the system for each degree of freedom q_i are expressed as

$$\begin{aligned}
Q_{x_G} & = F_x(t) + F_{rad_x}(\dot{x}, \dot{z}, \dot{\alpha}, t) + F_{visc_x}(t, x, z, \alpha, \dot{x}, \dot{z}, \dot{\alpha}) \\
Q_{z_G} & = F_z(t) + F_{rad_z}(\dot{x}, \dot{z}, \dot{\alpha}, t) + F_{visc_z}(t, x, z, \alpha, \dot{x}, \dot{z}, \dot{\alpha}) \\
Q_{\alpha} & = F_{\alpha}(t) + F_{rad_{\alpha}}(\dot{x}, \dot{z}, \dot{\alpha}, t) + F_{visc_{\alpha}}(t, x, z, \alpha, \dot{x}, \dot{z}, \dot{\alpha}) \\
Q_w & = -\frac{1}{2} \mu_h \eta (\nu \dot{w}) |\nu \dot{w}|
\end{aligned}$$

with η being the head loss coefficient corresponding to the restriction in the horizontal part of the TLCD. F and F_{rad} correspond to (4).

3. RESPONSE OF THE PASSIVE COUPLED SYSTEM

The Response Amplitude Operator (RAO), i.e. the ratio of the system's motion to the wave amplitude causing

that motion and presented over a range of (regular) wave periods (International Organization for Standardization, 2009), is employed as a quantitative tool for the rest of the study.

Now that we have defined the equations governing the motion of the whole system, we can simulate its behaviour and draw RAO diagrams. At this stage, the restriction coefficient η is constant.

3.1 Methodology

A simulation of the system is performed using a regular wave input, until the system has reached a periodic regime. This asymptotic regime defines the RAO. In this experiment, the TLCD is tuned to the natural pitch frequency of the structure ω_h yielding

$$L_e = \frac{2g}{\omega_h^2} = \frac{2g}{K_{h55}/M_{h55}}$$

M_D is set to 2% of the weight of the structure M_{h11} , ν is set to 4.3 to use the maximum space available, and e is designed to be the farthest possible from the centre of gravity i.e. $e = -10m$. The results have been obtained neglecting Morison's viscous drag force.

3.2 Results

We report RAOs for various values of the head loss coefficient η ranging from 0 to infinity. Results are presented in Fig.3. The case $\eta = 0$ corresponds to the absence of head loss as the liquid freely moves inside the tube. In this case, two resonance peaks are obtained. The case $\eta = +\infty$ corresponds to the stillness of the liquid in the tube ($w = 0$ at all times). A single peak close to the frequency of the structure can be observed. This latter case is, as expected, very similar to the case without TLCD as its inertia is very small compared to that of the structure. For intermediate values of η , one can see that all the RAOs have two points in common, one on each side of the natural period of the structure. These points will be referred to as *quasi-fixed* points in our discussion. The system is comparable to a mechanical double oscillator described by (Den Hartog, 1956) known as "damped vibration absorber". Changing the natural period of the TLCD can only shift the quasi-fixed points up and down the curve $\eta = +\infty$: when one point goes up and the other goes down. As discussed in (Den Hartog, 1956), the lowest amplitude is achieved when the two quasi fixed points are at the same height. A good tuning of the natural period of the TLCD and an adapted choice of η give a relatively flat gain for the response of the system.

The other parameters of the TLCD can also be optimized to lower the *quasi-fixed* points gain. This gain is represented in Fig.4. To determine the pitching amplitude in monochromatic loading we use linearised equations of motion, and follow the method proposed by (Wu et al., 2009) to linearize the quadratic head-loss coefficient for each ω considered. Again, we try to minimize the amplitude of the oscillations, we neglect the viscous effects in this procedure.

To determine the best design of TLCD, we simply use the `fmincon` optimisation function in MATLAB, with the following performance index to be minimized

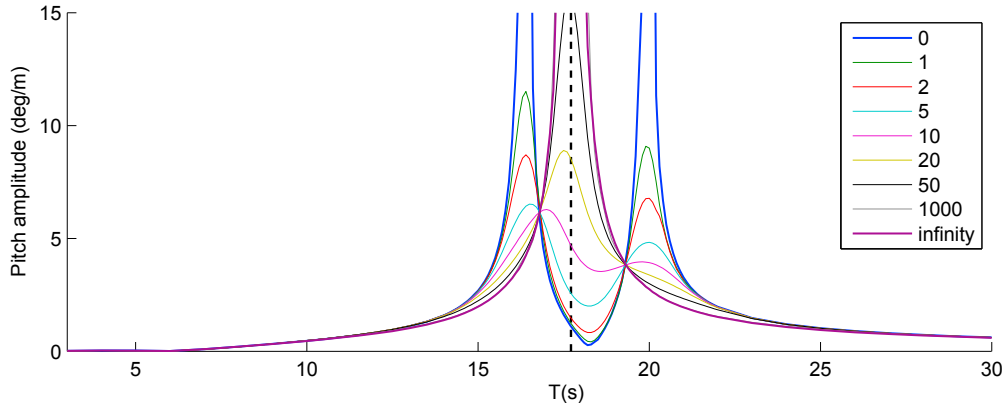


Fig. 3. RAO of pitching motion of the system for different values of η ranging from 0 to infinity.

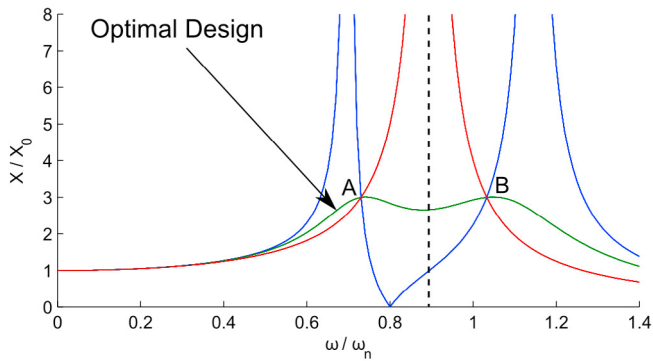


Fig. 4. Illustration of the response of a "Damped vibration absorber" with its *quasi-fixed* points, reproduced from (Den Hartog, 1956)

$$P.I.(L_h, L_v, \nu, \eta) = \max_{Tp \in [3;30]} (|\alpha|)$$

with $|\alpha|$ being the pitch magnitude in steady regime, for each period. This optimisation is done under constraints to account for the limited space available in the floater, and to guarantee that L_v is superior to a minimum guaranteeing that the liquid remains in the two vertical columns at all times. Here a minimum of 5 m has been chosen. As the natural period of the barge is close to the predominant period of extreme sea states (15s - 20s), we chose the performance index to damp this resonance. For a given site, we could use an adapted performance index to obtain a design best suited to the local sea state.

The results obtained with a wave height of 2 m are reported in Table 1.

L_h	L_v	ν	η
32.81 m	5 m	4.11	7.72

Table 1. Optimal TLCD parameters

4. SEMI-ACTIVE CONTROL

At the light of the previous results, one can consider changing the head loss coefficient η continually to achieve better performance. In the following, we define a semi active control strategy based on a simple linear quadratic

control design. The hydrodynamic model used to compute the radiation forces is (3).

4.1 Reduced model for design

To synthesise the control law we use a simplified model. We set x_G and z_G , i.e. surge and heave, to zero and we consider only the pitching and TLCD dynamics.

The linearised two degrees of freedom (pitch and liquid height) equations of motion of the system are of the form

$$M_1 \ddot{x}(t) + Kx(t) = E_1 (F_\alpha(t) + F_{rad_\alpha}(t)) + B_1 u(t) \quad (10)$$

with

$$F_{rad_\alpha}(t) = -\dot{\alpha}(t)\bar{B}_{h_{33}} - \ddot{\alpha}(t)\bar{A}_{h_{33}}$$

$\bar{B}_{h_{33}}$ and $\bar{A}_{h_{33}}$ being the (constant) values of $B_{h_{33}}(\omega)$ and $A_{h_{33}}(\omega)$ at the natural frequency of the structure, i.e. for $\omega = \omega_h$.

4.2 Semi-active control

Classically, a Linear Quadratic Regulator is considered resulting in a feedback gain K_c . To account for physical constraints, we clip the optimal strategy and define

$$\eta(t) = \text{sat}_{[\eta_{min}, \eta_{max}]} \left(\frac{2K_c X(t)}{\mu_h(\nu \dot{w})|\nu \dot{w}|} \right) \quad (11)$$

We choose η_{min} as zero, this corresponds to the fully opened restriction. We select η_{max} to be 1000, because, without loss of generality, as seen in Fig.3 the RAO obtained with this value of η is really close to the case $\eta = \infty$.

4.3 Results

Two series of simulations have been conducted. The hydrodynamic model is (4). The first simulation reproduces the response of the floater for 3 m high *monochromatic waves* which period is unknown to the algorithm and ranges from 3 to 30 s. The second series of simulations uses a JONSWAP *polychromatic* scenario with a peak period ranging from 3 to 30 s and with a 3 m significant wave height during 50 min. The optimal passive system presented in Section 3 serves as reference.

Table 2 reports the reduction of α standard deviation for the monochromatic and the JONSWAP polychromatic

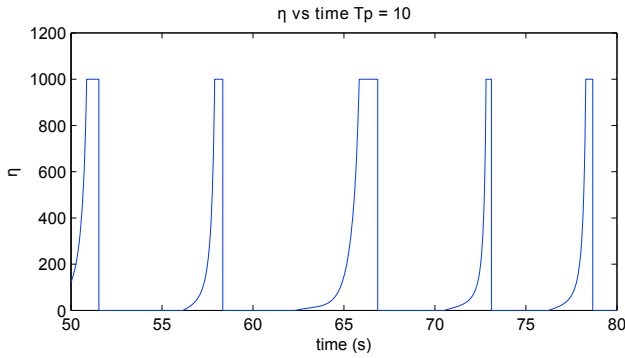


Fig. 5. η versus time for a polychromatic wave

waves described above. This variable is correlated to the mechanical load in the tower and should therefore be minimized.

	monochromatic	polychromatic
no TLCD	100	100
passive TLCD	59.4	72.7
semi-active TLCD	42.7	61.2

Table 2. pitch standard deviation compared to the floater without TLCD (%)

As expected, the semi-active control (11) reaches the best performance. This strategy is feasible, does not require any complicated nor powerful actuator. Further, the TLCD can behave like a passive system in case of mechanical or power failure. For these reasons, we believe that this semi-active solution has some good potential for applications.

5. CONCLUSION

In this paper, we have modelled and controlled a Floating Wind Turbine with a Tuned Liquid Column Damper. First, the pitch-surge-heave behaviour of the floater in the water has been detailed and, thanks to a Lagrangian approach, the TLCD (with its moving internal mass) has been incorporated in the system dynamics. Secondly, we have shown the limitations of the passive TLCD. Then, we have developed a reduced model of the system and a clipped optimal control law to overcome the limits. Finally we have used simulations to demonstrate the potential of the semi-active control to reduce further the pitching motion of the structure.

The control design under consideration is a simple saturated LQR. Naturally, one could study more advanced control designs, such as MPC (Mayne et al., 2000), especially to anticipate input constraints that have been only accounted for a posteriori, in a very suboptimal way.

Future works could also take into account valve dynamics to have a more realistic vision of the pitch reduction that could be achieved with a semi-active TLCD. For more realism, one should also consider the interaction between the wind and the rotor in the reduced model, and use a fully coupled hydro-aero-elastic software such as FAST or Principia Deeplines Wind for simulation. With those simulation tools, one could combine the use of the TLCD and the Blade Pitch Control strategies to further mitigate the tower load.

REFERENCES

- Butterfield, C.P., Musial, W., Jonkman, J., Scлавounos, P., and Wayman, L. (2007). *Engineering challenges for floating offshore wind turbines*. National Renewable Energy Laboratory Golden, CO, USA.
- Chang, C.C. and Hsu, C.T. (1998). Control performance of liquid column vibration absorbers. *Engineering Structures*, 20(7), 580–586. doi:10.1016/S0141-0296(97)00062-X.
- Chen, Y.H. and Ko, C.H. (2003). Active tuned liquid column damper with propellers. *Earthquake engineering and structural dynamics*, 32(10), 1627–1638. doi:10.1002/eqe.295.
- Christiansen, S., Tabatabaeipour, S.M., Bak, T., and Knudsen, T. (2013). Wave disturbance reduction of a floating wind turbine using a reference model-based predictive control. In *American Control Conference (ACC), 2013*, 2214–2219. IEEE. doi:10.1109/ACC.2013.6580164.
- Den Hartog, J.P. (1956). *Mechanical vibrations*. Courier Dover Publications.
- Di Matteo, A., Lo Iacono, F., Navarra, G., and Pirrotta, A. (2014). Direct evaluation of the equivalent linear damping for TLCD systems in random vibration for pre-design purposes. *International Journal of Non-Linear Mechanics*, 63, 19 – 30. doi:10.1016/j.ijnonlinmec.2014.03.009.
- Frahm, H. (1911). Results of trials of the anti-rolling tanks at sea. *Journal of the American Society for Naval Engineers*, 23(2), 571–597. doi:10.1111/j.1559-3584.1911.tb04595.x.
- Fried, L., Shukla, S., and Sawyer, S. (2012). Global wind report: annual market update 2011. *Global Wind Energy Council*.
- Fu, C. (2011). Active TLCD control of plane asymmetric buildings under earthquake excitation. *Acta Mechanica Sinica*, 27(5), 817–822. doi:10.1007/s10409-011-0504-2.
- Gao, H., Kwok, K., and Samali, B. (1997). Optimization of tuned liquid column dampers. *Engineering Structures*, 19(6), 476 – 486. doi:10.1016/S0141-0296(96)00099-5.
- Hasselmann, K., Barnett, T., Bouws, E., Carlson, H., Cartwright, D., Enke, K., Ewing, J., Gienapp, H., Hasselmann, D., Kruseman, P., et al. (1973). Measurements of wind-wave growth and swell decay during the Joint North Sea Wave Project (JONSWAP).
- Holden, C. and Fossen, T.I. (2012). A nonlinear 7-dof model for u-tanks of arbitrary shape. *Ocean Engineering*, 45, 22–37. doi:10.1016/j.oceaneng.2012.02.002.
- Holden, C., Galeazzi, R., Fossen, T.I., and Perez, T. (2009). Stabilization of parametric roll resonance with active u-tanks via lyapunov control design. In *European Control Conference (ECC)*, 4889–4894. IEEE.
- International Organization for Standardization (2009). Iso 13624-1-2009 petroleum and natural gas industries: Drilling and production equipment - part 1: Design and operation of marine drilling riser equipment.
- Jonkman, J.M. (2007). *Dynamics modeling and loads analysis of an offshore floating wind turbine*. Ph.D. thesis, National Renewable Energy Laboratory.
- Larsen, T.J. and Hanson, T.D. (2007). A method to avoid negative damped low frequent tower vibrations for a floating, pitch controlled wind turbine. In *Journal of Physics: Conference Series*, volume 75, 012073. IOP

- Publishing. doi:10.1088/1742-6596/75/1/012073.
- Mayne, D.Q., Rawlings, J.B., Rao, C.V., and Sokaert, P.O. (2000). Constrained model predictive control: Stability and optimality. *Automatica*, 36(6), 789–814. doi:10.1016/S0005-1098(99)00214-9.
- Moaleji, R. and Greig, A.R. (2006). Inverse control for roll stabilization of ships using active tanks. In *Proceedings of 7th Conference on Maneuvering and Control of Marine Craft*.
- Moaleji, R. and Greig, A.R. (2007). On the development of ship anti-roll tanks. *Ocean Engineering*, 34(1), 103 – 121. doi:10.1016/j.oceaneng.2005.12.013.
- Musial, W., Butterfield, S., Ram, B., et al. (2006). Energy from offshore wind. In *Offshore technology conference*, 1888–1898. Offshore Technology Conference.
- Namik, H. (2012). *Individual blade pitch and disturbance accommodating control of floating offshore wind turbines*. Ph.D. thesis, ResearchSpace @ Auckland.
- National Renewable Energy Laboratory (2012). *Renewable Energy Data Book*. U.S. Department of Energy.
- Newman, J.N. (1977). *Marine hydrodynamics*. MIT Press (Cambridge, Mass.).
- Perez, T. and Blanke, M. (2012). Ship roll damping control. *Annual Reviews in Control*, 36(1), 129–147. doi: 10.1016/j.arcontrol.2012.03.010.
- Wu, J.C., Chang, C.H., and Lin, Y.Y. (2009). Optimal designs for non-uniform tuned liquid column dampers in horizontal motion. *Journal of Sound and Vibration*, 326(1-2), 104 – 122. doi:10.1016/j.jsv.2009.04.027.
- Wu, J.C., Wang, Y.P., Lee, C.L., Liao, P.H., and Chen, Y.H. (2008). Wind-induced interaction of a non-uniform tuned liquid column damper and a structure in pitching motion. *Engineering Structures*, 30(12), 3555–3565. doi: 10.1016/j.engstruct.2008.05.029.
- Yalla, S. and Kareem, A. (2000). Optimum absorber parameters for tuned liquid column dampers. *Journal of Structural Engineering*, 126(8), 906–915. doi: 10.1061/(ASCE)0733-9445(2000)126:8(906).